Thermal Analysis of GTA Welding Electrodes

Maximum temperature occurs in midsection of tungsten electrode when operated at high currents

BY S. KOU AND M. C. TSAI

ABSTRACT. A steady-state, 1-dimensional heat flow model was developed to analyze the temperature distribution in tungsten 2% thoria electrodes during gas tungsten arc welding. The calculated results were in good agreement with the experimental ones reported by Savage, et al. The heat flow analysis also verified the observation of Savage, et al., that at high welding currents the maximum temperature occurs at an intermediate point between the electrode tip and the water-cooled collet. Furthermore, it was shown in this study that the overheating at this location is aggravated by the high electrical resistivity and low thermal conductivity associated with its high temperature, resulting ultimately in electrode failure by melting in half.

Introduction

Savage, et al. (Ref. 1), measured the temperature distribution in tungsten 2% thoria electrodes with an optical pyrometer during gas tungsten arc (GTA) welding. Various levels of welding current were used. For current levels near the upper end of the operating range of the electrode, an unusual phenomenon was observed, *i.e.*, the maximum temperature was always located at some intermediate point between the tip and the water-cooled collet, rather than at the tip.

To the best of our knowledge, the temperature distribution in a nonconsumable electrode during gas tungsten arc welding has not been analyzed so far, even though analytical equations for the temperature distribution in a consumable electrode during gas metal arc welding have been derived previously (Ref. 2).

The purpose of the present study is to verify the observations of Savage, et al., by conducting a heat flow analysis for the electrode during gas tungsten arc welding. Due to the fact that both the thermal and the electrical properties of the electrode material are strongly temperature dependent, simple analytical solutions are not possible to obtain. Consequently, a computer model based on the finite difference method was developed.

Numerical Method

Shown in Fig. 1 is a schematic sketch of the electrode portion of a GTA welding torch. The diameter of the electrode used by Savage, et al. (Ref. 1), was 2.38 mm (3/32 in.). In view of this rather small diameter, the temperature distribution is considered uniform in the radial direction of the electrode, *i.e.*, heat flow is considered 1-dimensional along the electrode axis.

With the help of Fig. 2, the following energy balance equation can be derived:

$$\frac{\partial}{\partial x}\left(k\frac{\partial T}{\partial x}\right) + Se - \frac{P}{A}\left[Q_R + h\,(T - T_a)\right] = 0 \qquad (1)$$

The explanation of the symbols in the above equation is given in nomenclature—Table 1. The first term in the left hand side of the equation represents the heat transfer due to conduction. The second term is the volumetric heat generation rate due to the electrical resistance of the electrode material. The third and fourth terms represent the heat loss from the electrode surface due to radiation and convection, respectively. The volumetric heat generation rate Se and the radiation heat loss Q_R can be expressed as follows:

$$Se = I^2\,\rho/A^2$$

and

$$Q_R = \sigma\,\epsilon\,(T^4 - T_w^4)$$

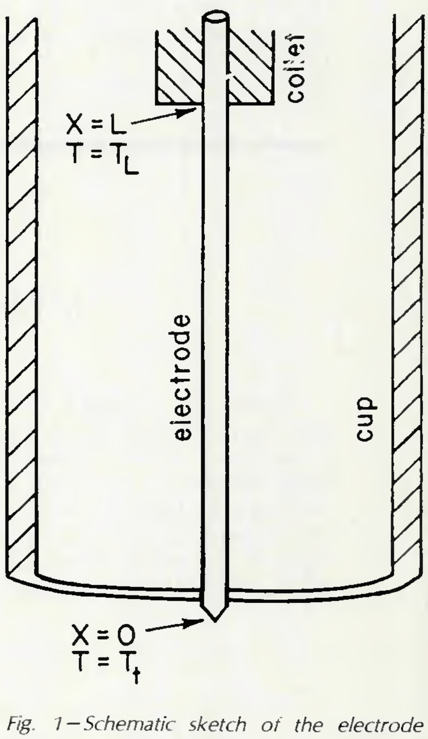

Fig. 1—Schematic sketch of the electrode portion of a GTA torch

S. KOU and M. C. TSAI are, respectively, Associate Professor and graduate student at the Department of Metallurgical and Mineral Engineering, University of Wisconsin, Madison, Wis.

The boundary conditions at the tip of the electrode and at the collet are as follows:

$$T = T_t \text{ at } x = o \quad (2)$$

and

$$T = T_L \text{ at } x = L \quad (3)$$

From equation (1), the following finite-difference equation can be derived for the temperature at node i:

$$T(i) = [C1 \cdot T(i-1) + C2 \cdot T(i+1) + C3 \cdot Se - C4 \cdot Q_R + C5]/(C1 + C2 + C6) \quad (4)$$

where

$$C1 = [k(i) + k(i-1)]/2$$
$$C2 = [k(i) + k(i+1)]/2$$
$$C3 = (\Delta X)^2$$
$$C4 = (\Delta X)^2\ P/A$$
$$C5 = (\Delta X)^2\ h\ T_a\ P/A$$
$$C6 = (\Delta X)^2\ h\ P/A$$

with

$$\Delta X = [X(i+1) - x(i-1)]/2$$

Since the electrode temperature is rather high (eq., up to 3500°K), the heat loss from the electrode surface is predominantly by radiation rather than by convection. Therefore, the convective heat transfer from the electrode surface to the argon shielding gas is negligible. Also, since the electrode temperature, T, is much higher than the temperature at the inside surface of the ceramic cup, T_w, $T^4 - T_w^4 \approx T^4$. Furthermore, since the diameter of the ceramic cup usually is much larger than that of the electrode (2.38 mm), the effect of the ceramic nozzle on the surface resistance of radiation is negligible. Finally, the transmittance of the shielding gas is essentially as one for most gases (Ref. 5).

The electrode tip temperature, T_t, was obtained by best fitting and extrapolating the measured temperature distribution in the electrode to its tip. The temperature at the electrode-collet interface, T_L, was obtained in a similar fashion, except in one case where L was shortened by 2 mm (0.08 in.) to improve accuracy.

The finite difference equation and the boundary conditions, *i.e.*, equations (2) to (4), were employed to solve the temperature distribution in the electrode. Twenty-one grid points were used. The successive over-relaxation method was used, with an over-relaxation parameter of about 1.2. A linear temperature distribution in the electrode was used as the initial guess for calculation. The physical properties were updated in each iteration of temperature calculation. The iterative procedure of temperature calculation was continued until the following convergence criterion was satisfied:

$$\left| \begin{matrix}\text{New} \\ T(i)\end{matrix} - \begin{matrix}\text{Old} \\ T(i)\end{matrix} \right|_{\text{maximum over all i}} \leqslant 1.0°K$$

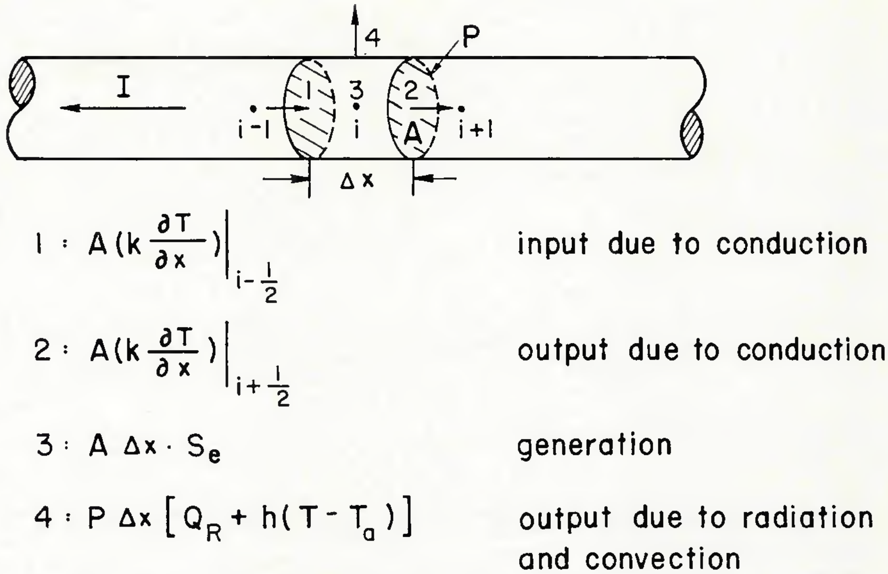

Fig. 2 — Control volume for energy balance equation

Physical Properties

The authors have attempted to locate the physical properties of tungsten 2% thoria through the computer-aided search but failed. Consequently, the physical properties of pure tungsten were used as an approximation.

Shown in Figs. 3 to 5 are the electrical resistivity (Ref. 3), thermal conductivity (Ref. 3) and emissivity (Ref. 4) of pure tungsten as a function of temperature (also see Table 2). The following three equations were used to approximate (less than 5% error) the temperature dependence of these physical properties from 400 to 3400°K:

$$\rho = -1.0 \times 10^{-5} + 3.333 \times 10^{-8}\ T$$
$$k = 9.890\ T^{-0.303}$$
$$\epsilon = -2.686 \times 10^{-2} + 1.820 \times 10^{-4}\ T - 2.195 \times 10^{-8}\ T^2$$

As a check for the effect of the 2% addition of thoria on the physical properties of tungsten, the electrical resistivity of tungsten 2% thoria was measured at the

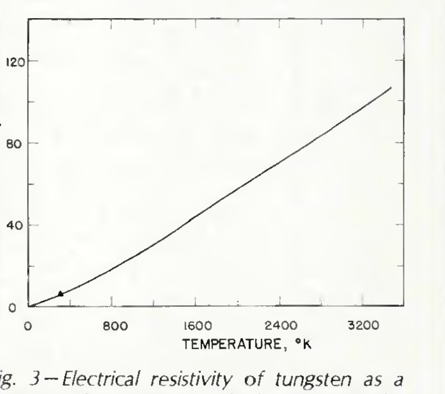

Fig. 3 — Electrical resistivity of tungsten as a function of temperature. The line indicates the approximation equation

Table 1—Nomenclature

- A Cross-sectional area of electrode [cm²]
- h heat transfer coefficient (W/cm² °K)
- I welding current [amp]
- k thermal conductivity of electrode [W/cm °K)
- L distance from electrode tip to collet [cm]
- P periphery of electrode [cm]
- Q_R radiation heat loss [W/cm²]
- Se volumetric heat generation rate due to electrical resistance [W/cm³]
- T temperature [°K]
- T_a temperature of argon gas [°K]
- T_L temperature at electrode-collet interface [°K]
- T_t temperature at electrode tip [°K]
- T_w temperature at the inside wall of ceramic cup [°K]
- x distance [cm]
- σ Stefan-Boltzmann constant = 5.67×10^{-12} [W/cm² °K⁴]
- ϵ emissivity of electrode
- ρ electrical resistivity of electrode [ohm-cm]

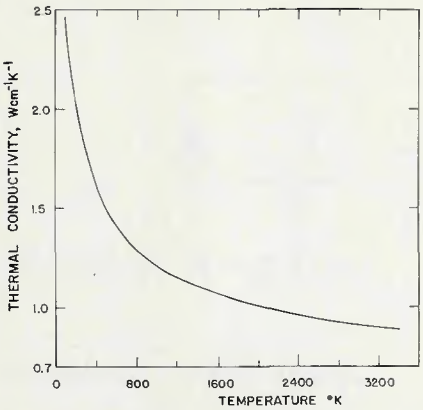

Fig. 4 — Thermal conductivity of tungsten as a function of temperature. The line indicates the approximation equation

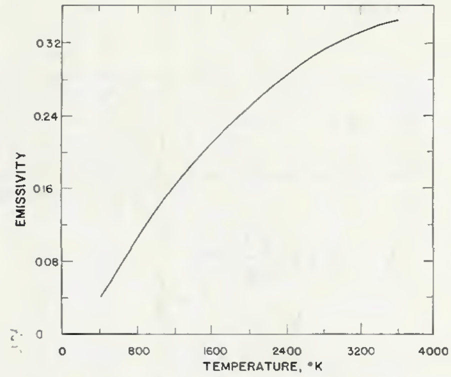

Fig. 5 — Emissivity of tungsten as a function of temperature

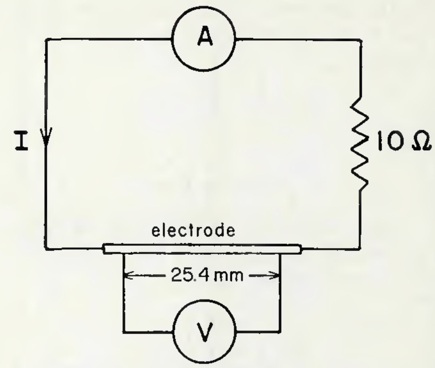

Fig. 6 — Circuit for measuring the electrical resistivity of tungsten 2% thoria electrode at room temperature

Table 2—Measured Electrical Resistivity of Tungsten 2% Thoria Electrode (2.38 mm diameter, 25.4 mm length) at Room Temperature

V (mV)	I (mA)	ρ (ohm-cm)
0.226	520.4	7.6×10^{-6}
0.227	523.2	7.6×10^{-6}
0.227	523.2	7.6×10^{-6}

room temperature using the circuit shown in Fig. 6. The current and voltage were measured with two Keithley 175 digital multimeters. As can be seen in Fig. 3, the measured electrical resistivity for tungsten 2% thoria at the room temperature is essentially the same as that of pure tungsten.

Results and Discussion

Figure 7 shows the calculated results for an electrode with a 120° tip angle and a 25.4 mm (1 in.) distance from the base of the conical tip to the collet. As shown, the agreement between the experimental and the calculated results is good.

The calculated temperature distribution at the welding current of 300 A exhibits a maximum temperature at an intermediate point between the tip and the collet, being consistent with the experimental observation of Savage, et al. (Ref. 1). At this high level of welding current, joule heating along the length of the electrode pushes its temperature to a high level. However, as pointed out by Savage, et al. (Ref. 1), in GTA welding using direct current with electrode negative, the tip end of the electrode is *cooled* by the thermionic emission of the electrons, while the collet end of the electrode is cooled by the cooling water. Consequently, the maximum temperature occurs in between the two ends.

According to Figs. 3 and 4, the electrical resistivity of the electrode increases with increasing temperature, while its thermal conductivity decreases with increasing temperature. Therefore, when the temperature at an intermediate point rises above those at the tip and the collet, more joule heating is produced at that point due to the higher local electrical resistivity. Furthermore, the lower local thermal conductivity makes it more difficult for the heat generated to be conducted away to cooler areas. These all tend to aggravate the local overheating problem and ultimately lead to electrode failure at high welding currents, by melting the electrode in half.

The fact that the electrode tip temperature, T_t, is essentially independent of the welding current is because the higher the welding current, the more electrons are emitted from the electrode tip per unit time, hence, the greater the cooling effect due to thermionic emission. Although it may not be necessary that T_t be exactly identical for various levels of welding current, a single value of T_t was used in the heat flow calculation. The temperature of the electrode at the collet, T_L, however, increases significantly with increasing welding current. Apparently, as the welding current increases, joule heating in the electrode increases rapidly (proportionally to I^2) and the collet has greater difficulty in cooling the electrode down.

As can be seen in Fig. 7, the calculated temperature is somewhat lower than the measured one in the high temperature range. This is probably due to the overes-

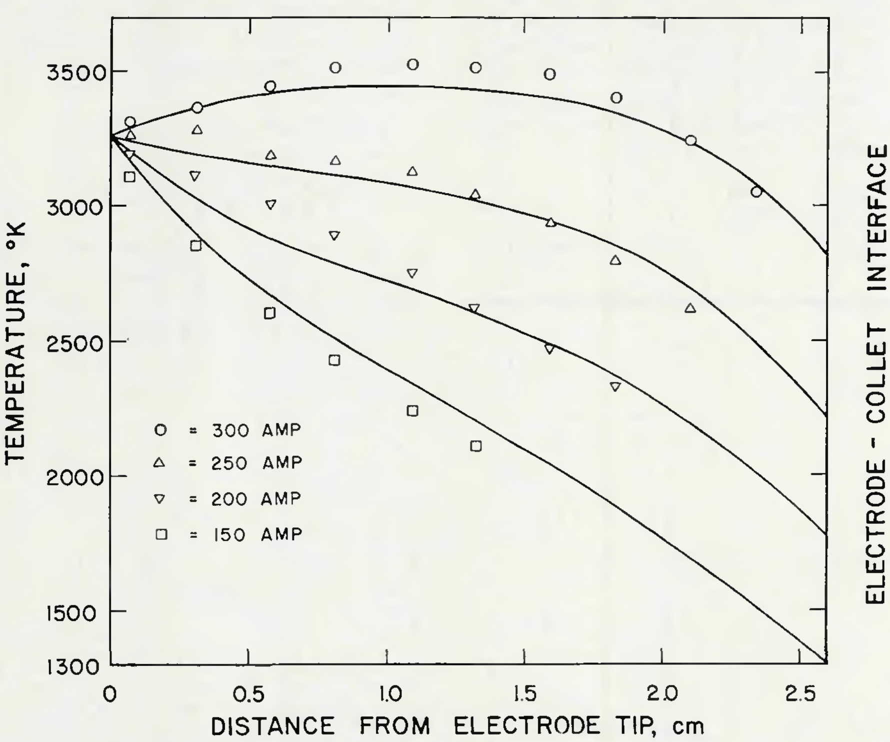

Fig. 7 — Comparison between calculated and observed temperature distributions in an electrode with a 120° tip angle and a 25.4 mm distance from the base of the conical tip to the collet

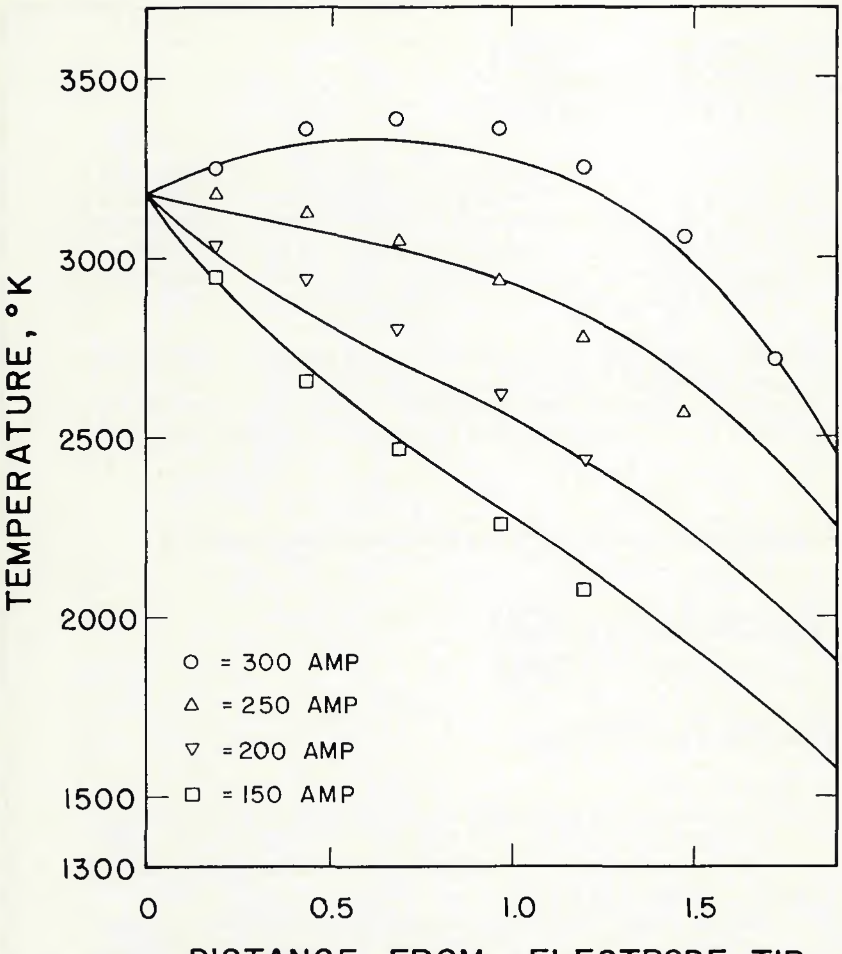

Fig. 8 — Comparison between calculated and observed temperature distributions in an electrode with a 60° tip angle and a 19.1 mm distance from the base of the conical tip to the collet

timated radiation heat loss, since the temperature at the inside surface of the ceramic cup, T_w, was neglected in the heat flow calculation. The discrepancy between the calculated temperature and the measured one at 150 A is likely to be due to the error in T_L caused by extrapolation.

Similar results of heat flow calculation are shown in Fig. 8 for an electrode with a 60° tip angle and a 19.1 mm (¾ in.) distance from the base of the conical tip to the collet. Again, the agreement between the experimental and the calculated results is good. The somewhat lower tip temperature in the present case is, perhaps, due to the greater ability of a sharper electrode tip to emit electrons.

Conclusion

1. A steady-state, 1-dimensional computer model was developed to describe heat flow in tungsten 2% thoria electrodes in GTA welding. Good agreement between the calculated and measured temperature profiles in the electrodes was obtained.
2. The model verified the observation of Savage, et al., that at high welding currents the maximum temperature occurs at an intermediate point between the electrode tip and the collet.
3. The overheating of the electrode at this location is aggravated by the high electrical resistivity and low thermal conductivity associated with its high temperature.

Acknowledgments

The authors gratefully acknowledge support for this study from the National Science Foundation, under NSF Grant No. DMR 8319341. The assistance by Professor D. C. Larbalestier in the measurement of the electrical resistivity is appreciated.

References

1. Savage, W. F., Strunck, S. S., and Ishikawa, Y. 1965. *Welding Journal* 44(11):489-s.
2. Myers, P. S., Uyehara, O. A., and Borman, G. L. 1967. Welding Research Council bulletin No. 123. Welding Research Council, New York.
3. *Thermophysical Properties of High Temperature Solid Materials*. 1967. Touloukian, Y. S., editor. MacMillan Company, New York, 1: pp. 1021 and 1025.
4. Yih, W. H., and Wang, C. T. 1979. *Tungsten*. Plenum Press, N.Y., p. 258.
5. Karlekar, B. V., and Desmond, R. M. 1977. *Engineering Heat Transfer*. West Publishing Company, N.Y., pp. 218 and 242.

WRC Bulletin 300
December 1984

Under the direction of the Steering Committee on Piping Systems of the Pressure Vessel Research Committee of the Welding Research Council, the Technical Committee on Piping Systems developed a document on criteria establishment describing their objectives and accomplishments, and three technical position documents that have an effect on the design of piping systems, entitled: 1) Technical Position on Criteria Establishment; 2) Technical Position on Damping Values for Piping Interim Summary; 3) Technical Position on Response Spectra Broadening; and 4) Technical Position on Industry Practice.

The Technical Position Documents have been submitted to the ASME Boiler and Pressure Vessel Code Committee and the U. S. Nuclear Regulatory Commission for their use.

The price of WRC Bulletin 300 is $14.00 per copy, plus $5.00 for postage and handling. Orders should be sent with payment to the Welding Research Council, Rm. 1301, 345 E. 47 St., New York, NY 10017.

WRC Bulletin 298
September 1984

Long-Range Plan for Pressure-Vessel Research—Seventh Edition
By the Pressure Vessel Research Committee

Every three years, the PVRC Long-Range Plan is updated. The Sixth Edition was widely distributed for review and comment. Updated problem areas have been suggested by ASME, API, EPRI and other organizations. Most of the problems in the Sixth Edition have been modified to meet current needs, and a number of new problems have been added to this Seventh Edition.

The list of "PVRC Research Problems" is composed of 58 research topics, divided into three groups relating to the three divisions of PVRC; i.e., materials, design and fabrication. Each project is outlined briefly in a project description, giving the title, statement of problem and objectives, current status and action proposed.

Because of budget limitations, PVRC will not be able to investigate all of these problems in the foreseeable future. Therefore, the cooperation and efforts of other groups in studying these areas is invited. If work is planned on one of the problems, PVRC should be informed in order to avoid duplication.

Publication of this bulletin was sponsored by the Pressure Vessel Research Committee of the Welding Research Council. The price of WRC Bulletin 298 is $14.00 per copy, plus $5.00 for postage and handling. Orders should be sent with payment to the Welding Research Council, Room 1301, 345 E. 47th St., New York, NY 10017.

WRC Bulletin 296
July 1984

Fitness-for-Service Criteria for Pipeline Girth-Weld Quality
By R. P. Reed, M. B. Kasen, H. I. McHenry, C. M. Fortunko and D. T. Read

In this report, criteria have been developed for applying fitness-for-service analyses to flaws in the girth welds of the Alaska Natural Gas Transmission System pipeline. A critical crack-opening-displacement elastic-plastic fracture mechanics model was developed and experimentally modified. Procedures for constructing curves based on this model are provided. A significantly improved ultrasonic method for detecting and dimensioning significant weld flaws was also developed.

Publication of this report was co-sponsored by the National Bureau of Standards and the Weldability Committee of the Welding Research Council. The price of WRC Bulletin 296 is $16.50 per copy, plus $5.00 for postage and handling. Orders should be sent with payment to the Welding Research Council, Room 1301, 345 E. 47 St., New York, NY 10017.